

Porous Cu(I) Triazolate Framework and Derived Hybrid Membrane with Exceptionally High Sensing Efficiency for Gaseous Oxygen

Si-Yang Liu, Xiao-Lin Qi, Rui-Biao Lin, Xiao-Ning Cheng, Pei-Qin Liao, Jie-Peng Zhang,* and Xiao-Ming Chen

Phosphorescent complexes of precious metal ions are widely studied as optical sensing materials for molecular oxygen. Combining the advantages of luminescent complexes and porous matrixes, porous coordination polymers show great potential for oxygen-sensing, although their sensitivity, requirement of precious metal, and device fabrication remain challenging issues. In this work, the photoluminescence and oxygen-sensing properties of the porous Cu(I) triazolate framework [Cu(detz)] (MAF-2, Hdetz = 3,5-diethyl-1,2,4-triazole) is studied in detail, which shows high chemical stability in moisture and water, very long phosphorescent lifetime (116 μ s) and large Stokes shift (14 562 cm^{-1}), as well as considerable oxygen permeability ($1.7 \times 10^{-11} \text{ mol cm}^{-1} \text{ s}^{-1} \text{ bar}^{-1}$) at ambient conditions, giving rise to exceptionally high luminescence quenching efficiency of 99.7% at 1 bar O_2 ($I_0/I_{100} = 356$) with a perfectly linear Stern-Volmer plot ($K_{SV} = 356 \text{ bar}^{-1}$, $R^2 = 0.9998$), fast response and good reversibility. Further, a counter-diffusion crystal-growth method was developed to fabricate MAF-2 thin films protected by silicone rubbers as the first example of soft membrane oxygen sensor based on coordination polymer or metal-organic framework, which exhibited extraordinary oxygen-sensing performance (limit of detection = 0.047 mbar) and outstanding mechanical property, as well as outstanding chemical stability even in an acidic atmosphere.

oxygen sensors based on luminescence quenching have attracted a great deal of attention for their high sensitivity and capability of online detections and non-invasion measurements.^[3] To fabricate a luminescence sensor, luminescent dyes should be immobilized on gas-permeable substrates, most of which are in the membrane form.^[4] It is worth pointing out that oxygen-sensing luminescent dyes usually perform very differently in the solution, bulk-solid, and thin-film states,^[5] and most sensing compounds have never become sensors.^[3]

Although some fluorescent materials have demonstrated high oxygen-sensing efficiencies,^[6] phosphorescent dyes, especially coordination complexes of precious metal ions (Pt, Ru, Au, Ir, Re, etc.), are still the most preferred choices for luminescent sensing,^[7] because phosphorescence based on triplet excited state has high quantum yield and luminescent intensity (for high sensitivity), long lifetime (for reducing the interference from scattered light and fluorescence background, by using time-resolved luminescence measurement), and large Stokes shift (for easy

separation of excitation and emission).^[8]

Porous coordination polymers (PCPs) are highly ordered arrays of metal complexes containing guest-accessible channels.^[9] Various functionalities, such as luminescent building blocks, can be rationally incorporated into PCPs.^[10] By virtue of their diverse and tunable structures, luminescent PCPs have emerged as promising sensing materials for solvent, vapor, and ion species.^[11] Recently, a few oxygen-sensing PCPs have been reported, which are mostly based on phosphorescent Ru(II) or Ir(III) metalloligands.^[12] So far, it is still very challenging to reduce the precious metal content and increase the oxygen-sensitivity of luminescent PCPs.^[6] In addition, bulk PCP crystals cannot be used directly in practical applications, especially as gas sensors. The loose powders are difficult to handle as a sensor unless they are processed or molded into applicable configurations such as membranes.^[13] Unlike molecular and macromolecular luminescent dyes, PCPs are generally fragile, crystalline and insoluble materials, which can be hardly made into soft membrane devices for sensing.^[14]

1. Introduction

Detecting the concentration of oxygen is of great practical significance,^[1] and high-sensitivity sensors are highly demanded for trace oxygen analyses in many environments that must be oxygen-free such as metallurgy, chemical industry, and so on.^[2] Optical

S.-Y. Liu, Dr. X.-L. Qi, R.-B. Lin, P.-Q. Liao,
Prof. Dr. J.-P. Zhang, Prof. Dr. X.-M. Chen
MOE Key Laboratory of Bioinorganic
and Synthetic Chemistry
State Key Laboratory of Optoelectronic
Materials and Technologies
School of Chemistry and Chemical Engineering
Sun Yat-Sen University
Guangzhou 510275, China
E-mail: zhangjp7@mail.sysu.edu.cn
Dr. X.-N. Cheng
Instrumental Analysis and Research Center
Sun Yat-Sen University
Guangzhou 510275, China



DOI: 10.1002/adfm.201401125

Luminescent Cu(I) complexes are cheap, noble-metal-free materials showing long-lifetime $^3\text{MLCT}$ (metal-to-ligand charge transferred triplet excited state) phosphorescence for oxygen-sensing.^[15] However, Cu(I) complexes, especially those in the solution states and dispersed in the porous structures, are well known for their instability toward air and humidity,^[16] which hinders their treatments and applications. Although some luminescent Cu(I)-based coordination polymers have been known,^[17] few of which showed permanent porosity,^[18] and none of which showed oxygen-sensing ability.

Metal azolate frameworks (MAFs) have been demonstrated as a unique type of coordination polymers with outstanding thermal and chemical stability even for Cu(I),^[19] which inspired us to explore the oxygen-sensing property of porous Cu(I)-based MAFs. In this work, we show that $[\text{Cu}(\text{detz})]$ (MAF-2, Hdetz = 3,5-diethyl-1,2,4-triazole, see Figure 1), a 3-connected **nbo-a** network with large cavities ($d = 7 \text{ \AA}$, void = 40%, BET and Langmuir surface areas: 539 and $807 \text{ m}^2 \text{ g}^{-1}$) and small apertures ($d = 1.5\text{--}3.6 \text{ \AA}$),^[18a] can serve as an extremely oxygen-sensitive phosphorescent material, which can be composited with silicon rubbers (SRs) to fabricate soft and robust membrane sensors with high sensitivity and outstanding stability in water and even acid vapor.

2. Results and Discussion

2.1. Synthesis and Characterization of MAF-2

Cu(I) 3,5-diethyl-1,2,4-triazolate was first designed and synthesized as a cubic phase (MAF-2c) by solvothermal *in situ* metal/ligand reaction of $\text{Cu}(\text{OH})_2$, aqueous ammonia, and propionitrile, but the poor reaction yield (10–15%) prevented characterization of many bulk properties.^[17c] Later, we established an efficient method for synthesis of trigonal phase MAF-2 by reacting Hdetz and $[\text{Cu}(\text{NH}_3)_2]\text{OH}$ in mixed ammonia/methanol under N_2 atmosphere at room temperature.^[18a] Compared

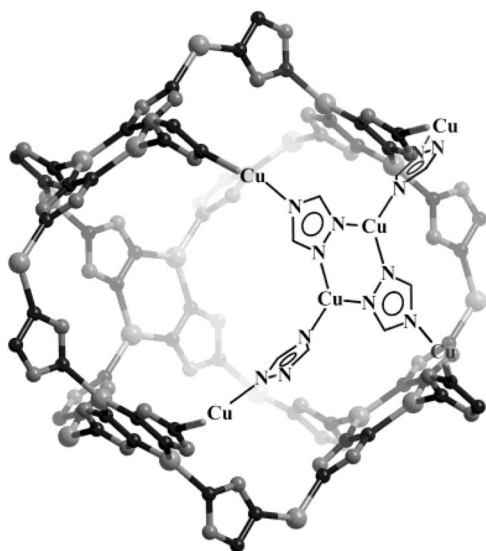


Figure 1. The cage structural unit of MAF-2 (the flexible ethyl groups of detz[−] ligands that block the apertures are omitted for clarity).

with MAF-2c, MAF-2 is guest-free with a less porous, shrunk structure. In this study, white microcrystalline powder of MAF-2 was synthesized by the direct method. Powder X-ray diffraction (PXRD) patterns and thermogravimetry (TG) analyses confirmed that the obtained sample was pure, guest-free, and highly thermostable (Figure S1 and S2).

The color and PXRD pattern of MAF-2 were unchanged in dry air (Figure S1 and S3). To examine the chemical stability under severer conditions, microcrystalline MAF-2 was exposed in saturated water vapor and immersed in water. In both cases, the samples turned light green after several days, but retained the original PXRD pattern even after 1 year. These phenomena indicated that MAF-2 was quite stable to either oxygen or water. Only in coexistence of oxygen and water, oxidation of the Cu(I) ions of MAF-2 can occur on the outer particle surface. It should be noted that, the chemical stabilities of MAF-2 toward air and water are much higher than conventional Cu(I) complexes, which should be attributed to its polymeric and hydrophobic framework structure consisting of strong metal-azolate bonds.^[19,20] These results should inspire the development of inexpensive sensing materials based on Cu(I) complexes.

2.2. Photoluminescence Properties of MAF-2

Bright $^3\text{MLCT}$ phosphorescence had been observed for MAF-2c in air.^[17c] However, microcrystalline MAF-2 is not luminescent in air, which is an indication of luminescence quenching by oxygen because framework distortion not likely changes the photoluminescence so much. Indeed, microcrystalline MAF-2 in vacuum showed broad and structureless emission spectra with excitation and emission maxima at 292 nm and 508 nm, respectively (Figure 2a), being similar to those reported for MAF-2c measured in air (Figure S4). The excitation wavelength of MAF-2 was shorter than common sensing materials, which can be ascribed to small π -conjugation system of detz[−] ligand. Although the short excitation wavelength may cause fluorescence interferences, the phosphorescence of MAF-2 possesses very large Stokes shift and long luminescence lifetime, which are highly demanded for practical applications. The Stokes shift between the excitation and emission peaks of MAF-2 (14562 cm^{-1}) was much larger than most of oxygen-sensing materials (ca. $4000\text{--}10000 \text{ cm}^{-1}$, see Table S1 and S2).^[5a,6,12,15,21] The luminescence lifetime of MAF-2 in vacuum was determined as $115.9(2) \text{ }\mu\text{s}$ (Figure 2b and S5), which is longer than most luminescent dyes used for oxygen-sensing (commonly $< 100 \text{ }\mu\text{s}$).^[22] For comparison, the luminescence lifetime of MAF-2c in air was reported to be ca. $1 \text{ }\mu\text{s}$.^[17c] Obviously, the guest molecules in MAF-2c prohibit efficient interaction between O_2 and the host framework, so that its luminescence is still observable in air.

The emission spectra of MAF-2 in different O_2 pressure (from vacuum to 1 bar) were measured (Figure 3a). The luminescence intensity of MAF-2 at 1 bar O_2 was $99.72(2)\%$ ($I_0/I_{100} = 355.8$) lower than that in vacuum. This value is significantly higher than those of PCPs and also higher than most molecular complexes (Table S1 and S2).^[2b,c] The oxygen-pressure-dependent luminescence intensity of MAF-2 was plotted by the Stern-Volmer equation (Equation(1));^[23]

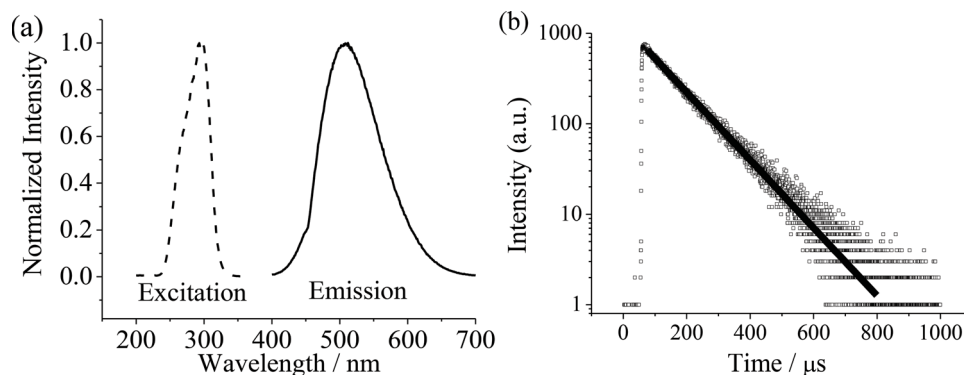


Figure 2. a) Photoluminescence spectra and b) decay profile (fitted by Equation (S1): $\tau_0 = 115.9(2)$ μs) of MAF-2 in vacuum.

$$\frac{I_0}{I} = \frac{\tau_0}{\tau} = 1 + \frac{4}{1000} \pi \sigma \alpha N_A \tau_0 D_{O_2} S_{O_2} P_{O_2} = 1 + K_{SV} P_{O_2} \quad (1)$$

where I_0/τ_0 and I/τ are the luminescent intensity/lifetime in the absence and presence of quencher, respectively, σ is the collision radius of the luminescent dye, α represents the probability that a collision leads to quenching, N_A is Avogadro's constant, D_{O_2} is the diffusion coefficients of oxygen, S_{O_2} is the oxygen solubility, P_{O_2} is the oxygen pressure, and K_{SV} is the quenching efficiency of the system.

The fitting plot exhibited excellent linearity with a very large slope of $K_{SV} = 356(1)$ bar⁻¹ (Figure 3b and S6),^[6,12b,15c,d,24] indicating MAF-2 has outstanding oxygen-sensing properties including wide liner range and extremely high sensitivity. Using excitation and detection wavelength of 292 and 508 nm, respectively, the luminescence intensity of microcrystalline MAF-2 was continuously recorded with stepwise change and cycling of O_2 (or air) pressure between 0 and 1 bar (Figure 4 and S7). After O_2 pressure changes, the luminescence intensity reaches equilibrium quickly, and there was no luminescence lost after 10 cycles, demonstrating fast response, good reversibility and high photochemical stability. O_2 sorption experiments for MAF-2 at 298 K demonstrated a solubility of *ca.* 0.12 mol L⁻¹ and a diffusion coefficient of *ca.* 1.4×10^{-7} cm² s⁻¹, giving a permeability of *ca.* 1.7×10^{-11} mol cm⁻¹ s⁻¹ bar⁻¹ (Figure S8), which is relatively high among common solid porous matrixes for oxygen sensor (10^{-13} – 10^{-11} mol cm⁻¹ s⁻¹ bar⁻¹).^[23,25]

2.3. Fabrication of Hybrid Membranes

Enlightened by the excellent oxygen-sensing performances of MAF-2, we tried to construct the corresponding sensors, which generally require the fabrication of thin membranes.^[26] Many SRs are soft, hydrophobic, transparent, oxygen-permeable, and nonluminescent polymers, which have been widely used as the porous matrixes for luminescence dyes in optical sensors.^[5a] We used a commercial SR, namely RTV-118, as the porous matrix and/or solid support for MAF-2. RTV-118 can be painted onto solid surfaces such as glass, silica and steel to form thin attached layers or molded into thin free-standing membranes. Obviously, MAF-2 crystals cannot be absorbed into SRs like small molecular dyes. Alternatively, the microcrystals can be attached on the membrane surfaces, either by mechanical coating or *in situ* synthesis/growth. In this study, the sensors were prepared by a counter-diffusion crystal-growth method which fabricates membranes with tightly attached and uniform microcrystal thin film.

As shown in Figure 5, the membrane sensors were prepared in three steps. First, The SR membranes were immersed in a CH₂Cl₂ solution of Hdetz, which swelled and absorbed the ligand solution. Second, in an aqueous ammonia/methanol solution of [Cu(NH₃)₂]OH, the CH₂Cl₂ solution of the ligand was extracted out the membranes and reacted with [Cu(NH₃)₂]OH to form MAF-2 microcrystals on the solid/liquid interface (Figure S9b). Third, although the crystal thin film attaches very tightly

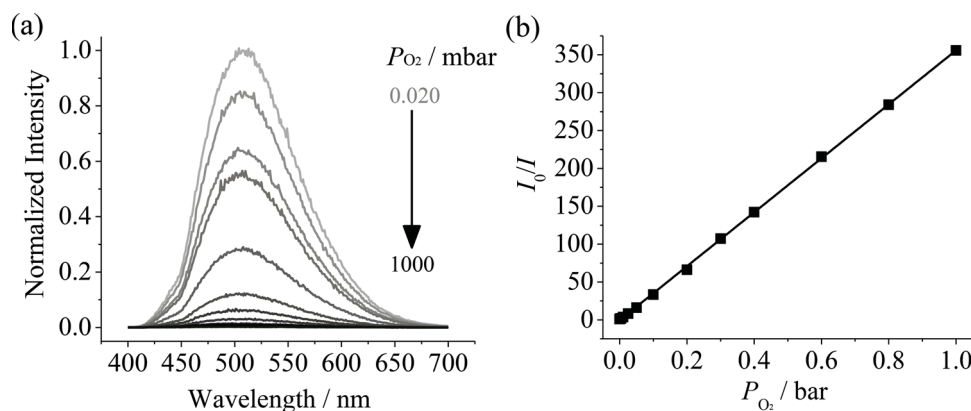


Figure 3. a) Emission spectra under different O_2 pressure and b) corresponding Stern-Volmer plot (fitted by Equation (1)) for MAF-2.

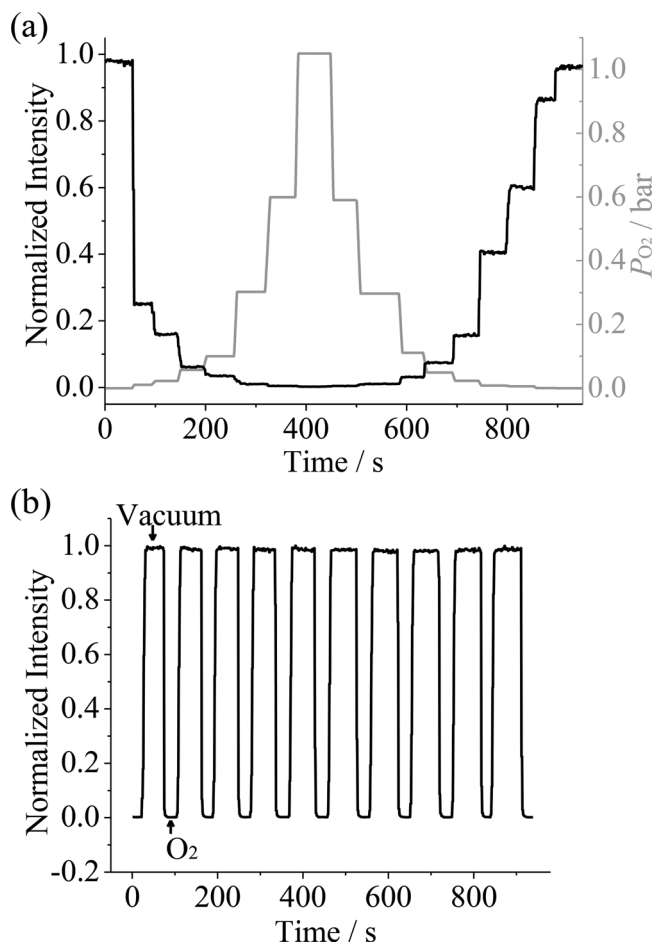


Figure 4. a) Time-dependent photoluminescence intensity of MAF-2 under stepwise change O₂ pressures and b) cycling between vacuum and 1 bar O₂ (excited by 292 nm, detected at 508 nm).

on the membrane surface, a thin layer of SR was coated above the MAF-2 crystals for further protection. Since RTV-118 releases acetic acid during vulcanization that can partially decompose MAF-2, a neutral dealcoholization SR, namely TSE-397-C, was adopted as the protective layer, which gave a sandwiched hybrid membrane hereafter denoted as MAF-2@SRs.

Scanning electron microscope (SEM) showed that the crystal diameters in bulk MAF-2 and MAF-2@SRs were *ca.* 1–15 and 3–4 μm , respectively (Figure S9), meaning that the *in situ* grown crystal thin film was more uniform.^[13a] TG showed that MAF-2@SRs decomposed at 400 °C and there was no obvious

weight loss at the decomposition temperature of MAF-2 (280 °C),^[18a] indicating that the hybrid membrane contained very small amounts of MAF-2 (Figure S2). When exposed in saturated water vapor and immersed in water, MAF-2@SRs showed higher stability than MAF-2. The color and PXRD pattern of MAF-2@SRs can be retained even in saturated vapor of hydrochloric acid (0.1 mol L⁻¹) for at least 1 month (Figure 6 and S10), being much improved than for microcrystalline MAF-2.

2.4. Oxygen-Sensing Properties of Hybrid Membranes

The luminescence and oxygen-sensing properties of the hybrid membranes were studied by similar measurements as for MAF-2. The luminescence spectra of MAF-2 and MAF-2@SRs were very similar (Figure S4). The Stern-Volmer plot of MAF-2@SRs below 0.1 bar exhibited perfect linearity and a very large slope of $K_{SV} = 213(1) \text{ bar}^{-1}$ (Figure 7a and S11a), which is suitable for low concentration oxygen sensing. As defined in a recent review by Wolfbeis *et al.*, the limit of detection (LOD) can be calculated at 1% quenching to ensure comparability and make it not subject to specific instrumental characteristics.^[27] In this context, the LOD of MAF-2@SRs was calculated to be $4.7 \times 10^{-2} \text{ mbar}$, which is only higher than a few state of the art optical oxygen sensors.^[28] Above 0.1 bar, the Stern-Volmer plot of MAF-2@SRs is nonlinear and levels off (Figure 7a and S11a). The luminescence intensity of MAF-2@SRs was quenched 99.14(3)% ($I_0/I_{100} = 116.8$) in 1 bar O₂ compared with that in vacuum (Figure S12). Such levels off Stern-Volmer plots were common in heterogeneous especially complex-polymer systems.^[5a] In the case of MAF-2@SRs, the polymer chains could fill some pores near the crystal surface of MAF-2 and prevent interaction with O₂, giving a downward Stern-Volmer plot with lower quenching efficiency.^[29] Although a linear relationship between signal intensity and analyte concentration is the best for device calibration,^[30] we found that the nonlinear Stern-Volmer plot of MAF-2@SRs can be well fitted by the following equation (Equation (2)):^[27]

$$\frac{I_0}{I} = \left(\frac{f_1}{1 + K_{SV1}P_{O_2}} + \frac{f_2}{1 + K_{SV2}P_{O_2}} \right)^{-1} \quad (2)$$

where f_1 and f_2 are the fractions of the two sites that are quenched with the quenching efficiencies K_{SV1} and K_{SV2} , respectively.

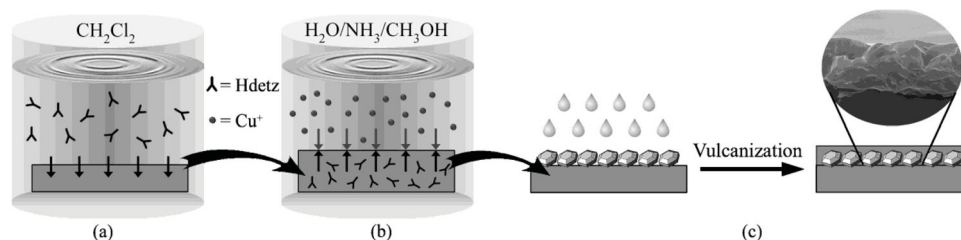


Figure 5. Schematic illustration of the fabrication method of the hybrid membrane. a) Absorption of a CH₂Cl₂ solution of Hdetz into an SR membrane, b) extraction of the CH₂Cl₂ solution of Hdetz from the membrane with an aqueous ammonia/methanol solution of [Cu(NH₃)₂]OH (the ligand and Cu(II) ion react on the membrane surface to generate MAF-2 crystals), and c) covering the surface crystals with an SR protection layer.

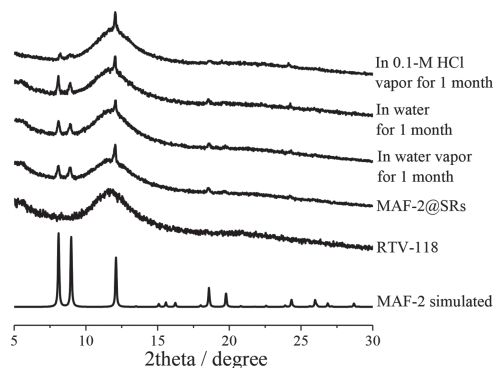


Figure 6. PXRD patterns of MAF-2@SRs treated at different chemical conditions.

The fitting results showed that one of the two quenching constants must be close to zero, giving fitting parameters $f_1 = 0.995(6)$, $K_{SV1} = 264(7) \text{ bar}^{-1}$, $f_2 = 0.005(5)$, $K_{SV2} = 0 \text{ bar}^{-1}$ (Figure 7a and S11b), indicating that there were 0.5% MAF-2 which cannot be quenched by O_2 . These data demonstrated

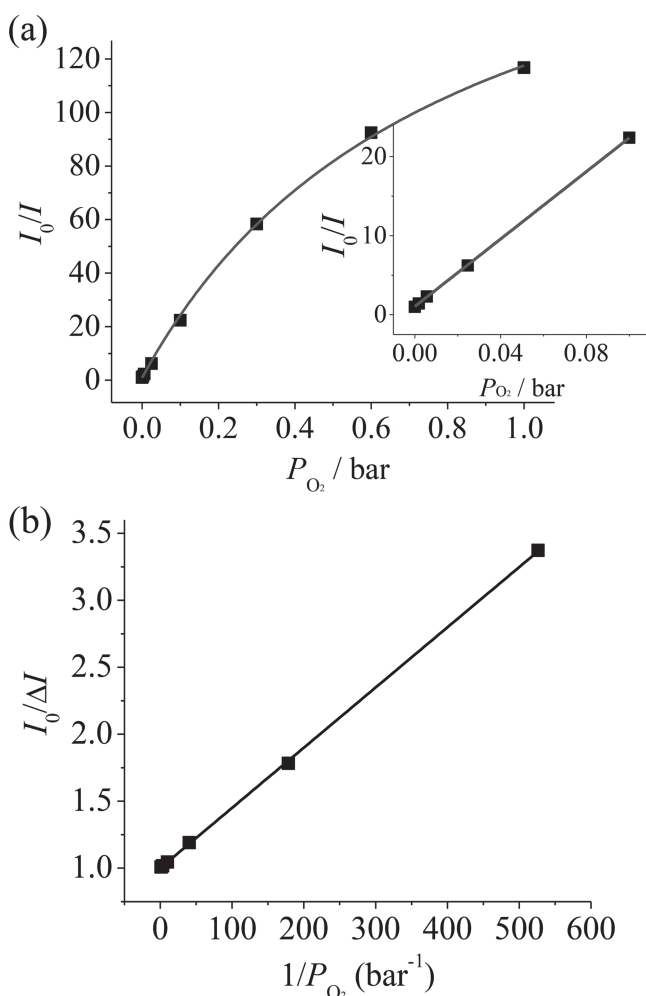


Figure 7. a) Stern-Volmer plot (fitted by Equation (2)); inset: low-pressure part fitted by Equation (1) and b) modified Stern-Volmer plot (fitted by Equation (3)) of MAF-2@SRs (excited by 292 nm, detected at 512 nm).

that even minute amount of unquenched or hardly-quenched component can lead to dramatically nonlinearity in the Stern-Volmer plots. By fixing $K_{SV2} = 0$, Equation (2) can be rearranged to a linear format (Equation (3)).^[30]

$$\frac{I_0}{\Delta I} = \frac{1}{fK_{SV}P_{O_2}} + \frac{1}{f} \quad (3)$$

where $\Delta I = I_0 - I$, and f is the fraction of the components which are accessible to the quencher (O_2 molecules). The fitting results exhibited good linearity, with $K_{SV} = 223(2) \text{ bar}^{-1}$ and $f = 0.999(5)$ (Figure 7b and S11c). The resulted K_{SV} values of the two equations were different because the coefficients of Equation (2) and Equation (3) were mainly controlled by the low- and high-pressure parts of data, respectively. Nevertheless, both K_{SV} values were larger than most hybrid oxygen sensors (Table S1 and S2).^[21]

Although the MAF-2 crystals are covered by SRs, MAF-2@SRs can also rapidly respond to O_2 pressure changes (Figure S13a). The luminescence intensity can reach equilibrium in less than 1 s, and no obvious luminescence intensity loss could be observed after switching the atmosphere between vacuum and 1 bar O_2 or air for 10 cycles (Figure S13b and S13c). More practical performance of MAF-2@SRs were shown in Video S1 and Figure 8, which demonstrated the fast response, drastic quenching, and good reversibility of the soft, free-standing membrane. It should be noted that, soft membrane oxygen sensor based on coordination polymers or metal-organic frameworks has not been reported in the literature.

3. Conclusion

In summary, based on the porous Cu(I) diethyltrizolate framework MAF-2, optical oxygen-sensing properties were observed for the first time in Cu(I)-based PCPs and also in noble-metal-free phosphorescent PCPs. This study reveal that MAF-2 has fairly high stability in air and water, bright phosphorescence with very long lifetime and large Stokes shift, as well as high uptake and fast sorption kinetics for oxygen at ambient conditions, which give rise to the exceptionally high oxygen-sensing efficiency. More importantly, a counter-diffusion crystal-growth method has been developed to fabricate uniform MAF-2 thin films in silicon rubbers to construct solid-attached or free-standing, and mechanically soft and robust membrane sensors, which not only preserve the oxygen-sensing characteristics but

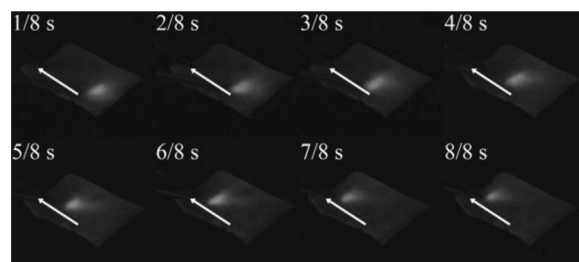


Figure 8. Photographs (screenshots in Video S1) of MAF-2@SRs (in air under 254-nm UV light) under a moving needle (arrows indicate the trajectory of the pinhead) blowing N_2 .

also further improve the chemical stability of the luminescent PCP. These results may open up new prospects for low-cost, sensitive, and durable sensory materials and devices.

4. Experimental Section

Materials and Methods: Commercially available reagents and solvents were used as received without further purification. The $[\text{Cu}(\text{NH}_3)_2]\text{OH}$ in mixed ammonia/methanol solution was prepared by add hydrazine hydrate into the mixed ammonia/methanol solution of $\text{Cu}(\text{OH})_2$. The ligand Hdetz and microcrystalline powder of MAF-2 were synthesized according to the literature methods.^[18a] Room temperature vulcanization SRs RTV-118 and TSE-397-C were obtained from Momentive Performance Materials Co., Ltd. PXRD patterns were performed on a Bruker D8 ADVANCE X-ray powder diffractometer ($\text{Cu-K}\alpha$). Thermogravimetry measurements were performed on a TA Q50 instrument under nitrogen atmosphere. Gas sorption isotherms were measured on a volumetric adsorption apparatus (Micrometrics ASAP 2020M). The sample (weight about 200 mg) was *in situ* evacuated under high vacuum at 353 K for 12 h prior to the sorption measurements. For SEM, the samples were sputter coated with gold and examined with a Quanta 400 field-emitted SEM device.

Fabrication of Hybrid Membranes: RTV-118 was placed into a plexiglas clamping apparatus to modulate the thickness of the resultant membranes, then cured with atmospheric moisture at room temperature for 24 h to give transparent membranes (thickness ≈ 0.2 mm), which were immersed in a CH_2Cl_2 solution of Hdetz (0.5 mol L^{-1}) for 10 min. The swelled membranes were taken out and put into a slowly stirring (60 rpm) solution of $[\text{Cu}(\text{NH}_3)_2]\text{OH}$ (0.1 mol L^{-1}) in aqueous ammonia/methanol (1:1, 100 mL) immediately. After 5 min, the shrunk and frosted membranes were taken out, washed by methanol to give MAF-2/RTV-118 membranes. A CH_2Cl_2 solution of TSE-397-C (10 wt%) was sprayed onto these membranes using an air brush, then the membranes were dried in air for 10 min to give semitransparent sandwiched membranes denoted as MAF-2@SRs.

Photoluminescence Measurement: Steady state photoluminescence spectra and lifetime measurements were performed at room temperature on an Edinburgh FLS920 spectrometer equipped with a continuous Xe900 Xenon lamp and an F900 microsecond flash lamp. All instrument parameters such as excitation split, emission split, scanning speed were fixed for all measurements. *In situ* oxygen responding luminescence was measured in a sealed chamber equipped with quartz windows and a three-way valve which connects the chamber to a vacuum pump and an O_2 cylinder or atmosphere. The chamber was subjected to dynamic vacuum for 1 h before photoluminescence measurements for oxygen-sensing. The luminescence spectra were measured after the targeted oxygen pressure was kept for 30 s. In the cycling reversibility experiment, the pressure was vacuumed to 0.01–0.03 mbar.

Supporting Information

Thermogravimetry curves, PXRD patterns, additional figures, photoluminescence data, SEM images, gas sorption data, and a video of the luminescence oxygen sensor. Supporting Information is available from the Wiley Online Library or from the author.

Acknowledgements

This work was supported by the “973 Project” (2012CB821706 and 2014CB845602) and NSFC (21225105, 21121061, and 21371181).

Received: April 8, 2014

Revised: May 22, 2014

Published online: July 14, 2014

- [1] B. Valeur, M. N. Berberan-Santos, in *Molecular Fluorescence*, Wiley-VCH, Weinheim, Germany **2012**, pp. 409.
- [2] a) E. T. Turkdogan, R. J. Fruehan, *Can. Metall. Q.* **1972**, *11*, 371; b) S. Nagl, C. Baleizão, S. M. Borisov, M. Schäferling, M. N. Berberan-Santos, O. S. Wolfbeis, *Angew. Chem., Int. Ed.* **2007**, *46*, 2317; c) C. Baleizão, S. Nagl, M. Schäferling, M. N. Berberan-Santos, O. S. Wolfbeis, *Anal. Chem.* **2008**, *80*, 6449.
- [3] M. I. Stich, L. H. Fischer, O. S. Wolfbeis, *Chem. Soc. Rev.* **2010**, *39*, 3102.
- [4] D. E. Achatz, R. J. Meier, L. H. Fischer, O. S. Wolfbeis, *Angew. Chem., Int. Ed.* **2011**, *50*, 260.
- [5] a) E. R. Carraway, J. N. Demas, B. A. DeGraff, J. R. Bacon, *Anal. Chem.* **1991**, *63*, 337; b) J. R. Bacon, J. N. Demas, *Anal. Chem.* **1987**, *59*, 2780.
- [6] R.-B. Lin, F. Li, S.-Y. Liu, X.-L. Qi, J.-P. Zhang, X.-M. Chen, *Angew. Chem., Int. Ed.* **2013**, *52*, 13429.
- [7] D. Parker, *Coord. Chem. Rev.* **2000**, *205*, 109.
- [8] a) Y. Feng, J. Cheng, L. Zhou, X. Zhou, H. Xiang, *Analyst* **2012**, *137*, 4885; b) Q. Zhao, F. Li, C. Huang, *Chem. Soc. Rev.* **2010**, *39*, 3007; c) C. Ulbricht, B. Beyer, C. Friebe, A. Winter, U. S. Schubert, *Adv. Mater.* **2009**, *21*, 4418.
- [9] S. R. Batten, N. R. Champness, X.-M. Chen, J. Garcia-Martinez, S. Kitagawa, L. Öhrström, M. O’Keeffe, M. Paik Suh, J. Reedijk, *Pure Appl. Chem.* **2013**, *85*, 1715.
- [10] a) Y.-J. Cui, Y.-F. Yue, G.-D. Qian, B.-L. Chen, *Chem. Rev.* **2012**, *112*, 1126; b) C.-Y. Sun, X.-L. Wang, X. Zhang, C. Qin, P. Li, Z.-M. Su, D.-X. Zhu, G.-G. Shan, K.-Z. Shao, H. Wu, J. Li, *Nat. Commun.* **2013**, *4*.
- [11] a) L. E. Kreno, K. Leong, O. K. Farha, M. Allendorf, R. P. Van Duyne, J. T. Hupp, *Chem. Rev.* **2012**, *112*, 1105; b) M. D. Allendorf, C. A. Bauer, R. K. Bhakta, R. J. T. Houk, *Chem. Soc. Rev.* **2009**, *38*, 1330; c) B. Chen, S. Xiang, G. Qian, *Acc. Chem. Res.* **2010**, *43*, 1115; d) H.-L. Jiang, Y. Tatsu, Z.-H. Lu, Q. Xu, *J. Am. Chem. Soc.* **2010**, *132*, 5586; e) K. C. Stylianou, R. Heck, S. Y. Chong, J. Bacsá, J. T. A. Jones, Y. Z. Khimyak, D. Bradshaw, M. J. Rosseinsky, *J. Am. Chem. Soc.* **2010**, *132*, 4119; f) N. Yanai, K. Kitayama, Y. Hijikata, H. Sato, R. Matsuda, Y. Kubota, M. Takata, M. Mizuno, T. Uemura, S. Kitagawa, *Nat. Mater.* **2011**, *10*, 787; g) S. Pramanik, C. Zheng, X. Zhang, T. J. Emge, J. Li, *J. Am. Chem. Soc.* **2011**, *133*, 4153; h) D. Liu, K. Lu, C. Poon, W. Lin, *Inorg. Chem.* **2013**, *53*, 1916.
- [12] a) Z. Xie, L. Ma, K. E. deKrafft, A. Jin, W. Lin, *J. Am. Chem. Soc.* **2009**, *132*, 922; b) M.-L. Ho, Y.-A. Chen, T.-C. Chen, P.-J. Chang, Y.-P. Yu, K.-Y. Cheng, C.-H. Shih, G.-H. Lee, H.-S. Sheu, *Dalton Trans.* **2012**, *41*, 2592; c) J. An, C. M. Shade, D. A. Changelis-Czegan, S. Petoud, N. L. Rosi, *J. Am. Chem. Soc.* **2011**, *133*, 1220; d) S. M. Barrett, C. Wang, W. Lin, *J. Mater. Chem.* **2012**, *22*, 10329; e) X. L. Qi, S. Y. Liu, R. B. Lin, P. Q. Liao, J. W. Ye, Z. Lai, Y. Guan, X. N. Cheng, J. P. Zhang, X. M. Chen, *Chem. Commun.* **2013**, *49*, 6864.
- [13] a) D. Bradshaw, A. Garai, J. Huo, *Chem. Soc. Rev.* **2012**, *41*, 2344; b) B. Liu, *J. Mater. Chem.* **2012**, *22*, 10094.
- [14] D. Zacher, O. Shekhah, C. Wöll, R. A. Fischer, *Chem. Soc. Rev.* **2009**, *38*, 1418.
- [15] a) L. Shi, B. Li, *Eur. J. Inorg. Chem.* **2009**, *2009*, 2294; b) L. Shi, B. Li, S. Yue, D. Fan, *Sens. Actuators, B* **2009**, *137*, 386; c) Y. Wang, B. Li, Y. Liu, L. Zhang, Q. Zuo, L. Shi, Z. Su, *Chem. Commun.* **2009**, 5868; d) C. S. Smith, C. W. Branham, B. J. Marquardt, K. R. Mann, *J. Am. Chem. Soc.* **2010**, *132*, 14079; e) J. Haitao, Y. Huilin, L. Fan, L. Yang, *J. Lumin.* **2012**, *132*, 198; f) C. S. Smith, K. R. Mann, *J. Am. Chem. Soc.* **2012**, *134*, 8786; g) J. Jia, Y. Tian, Z. Li, *Synth. Met.* **2011**, *161*, 1377.
- [16] M. Grzywa, C. Geßner, D. Denysenko, B. Bredenkötter, F. Gschwind, K. M. Fromm, W. Nitek, E. Klemm, D. Volkmer, *Dalton Trans.* **2013**, *42*, 6909.

- [17] a) X.-C. Shan, F.-L. Jiang, D.-Q. Yuan, H.-B. Zhang, M.-Y. Wu, L. Chen, J. Wei, S.-Q. Zhang, J. Pan, M.-C. Hong, *Chem. Sci.* **2013**, 4, 1484; b) S.-Z. Zhan, M. Li, S. W. Ng, D. Li, *Chem. Eur. J.* **2013**, 19, 10217; c) J.-P. Zhang, Y.-Y. Lin, X.-C. Huang, X.-M. Chen, *J. Am. Chem. Soc.* **2005**, 127, 5495; d) J. P. Zhang, Y. Y. Lin, X. C. Huang, X. M. Chen, *Dalton Trans* **2005**, 3681.
- [18] a) J.-P. Zhang, X.-M. Chen, *J. Am. Chem. Soc.* **2008**, 130, 6010; b) F. Wang, R. Yu, Q.-S. Zhang, Z.-G. Zhao, X.-Y. Wu, Y.-M. Xie, L. Qin, S.-C. Chen, C.-Z. Lu, *J. Solid State Chem.* **2009**, 182, 2555; c) Y. Yu, X.-M. Zhang, J.-P. Ma, Q.-K. Liu, P. Wang, Y.-B. Dong, *Chem. Commun.* **2014**, 50, 1444; d) J.-P. Zhang, S. Kitagawa, *J. Am. Chem. Soc.* **2008**, 130, 907.
- [19] J.-P. Zhang, Y.-B. Zhang, J.-B. Lin, X.-M. Chen, *Chem. Rev.* **2011**, 112, 1001.
- [20] H. Furukawa, K. E. Cordova, M. O'Keeffe, O. M. Yaghi, *Science* **2013**, 341.
- [21] a) L. Huynh, Z. Wang, J. Yang, V. Stoeva, A. Lough, I. Manners, M. A. Winnik, *Chem. Mater.* **2005**, 17, 4765; b) X.-D. Wang, X. Chen, Z.-X. Xie, X.-R. Wang, *Angew. Chem., Int. Ed.* **2008**, 47, 7450; c) B. W.-K. Chu, V. W.-W. Yam, *Langmuir* **2006**, 22, 7437.
- [22] H. Xiang, J. Cheng, X. Ma, X. Zhou, J. J. Chruma, *Chem. Soc. Rev.* **2013**, 42, 6128.
- [23] X. Lu, M. A. Winnik, *Chem. Mater.* **2001**, 13, 3449.
- [24] C. S. Smith, K. R. Mann, *Chem. Mater.* **2009**, 21, 5042.
- [25] C. N. Jayarajah, A. Yekta, I. Manners, M. A. Winnik, *Macromolecules* **2000**, 33, 5693.
- [26] C. McDonagh, C. S. Burke, B. D. MacCraith, *Chem. Rev.* **2008**, 108, 400.
- [27] X.-D. Wang, O. S. Wolfbeis, *Chem. Soc. Rev.* **2014**, 43, 3666.
- [28] a) Precise Sening GmbH Sensor probes for oxygen, <http://www.presens.de>, Accessed April 2014; b) S. M. Borisov, P. Lehner, I. Klimant, *Anal. Chim. Acta* **2011**, 690, 108; c) B.-H. Han, I. Manners, M. A. Winnik, *Chem. Mater.* **2005**, 17, 3160; d) S. Kochmann, C. Baleizão, M. N. Berberan-Santos, O. S. Wolfbeis, *Anal. Chem.* **2013**, 85, 1300.
- [29] W. Xu, R. C. McDonough, B. Langsdorf, J. N. Demas, B. A. DeGraff, *Anal. Chem.* **1994**, 66, 4133.
- [30] W. Wu, S. Ji, W. Wu, H. Guo, X. Wang, J. Zhao, Z. Wang, *Sens. Actuators, B* **2010**, 149, 395.